Environment Protection Engineering

Vol. 47 2021 No. 2

DOI:10.37190/epe210205

LAMYA ARROUG (ORCID: 0000-0001-5698-7121)[1]

MOHAMED ELAATMANI (ORCID: 0000-0002-0986-0045)[1]

ABDELOUAHAD ZEGZOUTI (ORCID: 0000-0002-4447-3876)[1]

MOHAMED AFQIR (ORCID: 0000-0002-2636-8810)[1]

MOUNSIF IBNOUSSINA (ORCID: 0000-0003-0733-687X)[2]

MOHAMMED AIT BABRAM (ORCID: 0000-0003-1958-466X)[3]

EFFECTS OF LONG-TERM STORAGE OF PHOSPHATE SLUDGES ON THEIR PHYSICOCHEMICAL PROPERTIES, THE DISTRIBUTION AND MOBILITY OF HEAVY METALS, AND ACID GENERATION

Some phosphate sludges (Ps) were collected in 2009, 2014, and 2018. Results of their analyses by X-ray diffraction (XRD), Fourier transform infrared spectroscopy (FTIR), scanning electron microscopy (SEM-SED), differential thermal and thermogravimetric analyses (TG-DTA) and X-ray fluorescence spectrometry (XRF) confirmed that the Ps are highly carbonated. Descriptive and exploratory statistical procedures for heavy metals (HM) concentrations and chemical parameters were performed and revealed the differences between the Ps of three different ages. The results indicate that there are three sources responsible for the behavior of Ps over years: common origin and accumulation of HM and solar radiation exposure. The sequential extraction shows that the residual fractions of Cd, Ni, Zn, Pb, and Cr were predominant. The mobility factor was quite low and did not change over the years, except for Cd. The net acid generation pH for the three samples was greater than 4.5 classifying the Ps as non-acid-generating.

[1]Laboratory of Materials Science and Process Optimization, Cadi Ayyad University, Semlalia Faculty of Science, Marrakech, Morocco, corresponding author, email address: Lamya.arroug@gmail.com

[2]Laboratory of Geodynamics, Geomatics, and Geotechnics, Cadi Ayyad University, Semlalia Faculty of Science, Marrakech, Morocco.

[3]Department of Mathematics of the Faculty of Science and Technology, Cadi Ayyad University, Marrakech, Morrocco.

1. INTRODUCTION

Every year, the process of mining itself generates large amounts of residues worldwide. These amounts are expected to strongly increase up to 11 billion tons per year, with an associated environmental impact. The mining extraction process sorting through large amounts of data to extract useful information, important values, or key relationships. In this regard, the view that more can be done to enhance the ability of the site extractive sector to manage the environment is accompanied by a process of optimization and impact assessment.

The phosphate mining sector also faces many environmental problems due to the huge amounts of tailings generated by mining. Extracted phosphate requires mechanical preparation of sifting and crushing. It is then sent toward the industrial washing plant to be treated. However, the raw material physical and chemical treatment releases minerals components when separated from impurities (silicates and carbonates). During the washing process, huge amounts of sludge and associated residues are generated. These tailings are stored in large ponds, without any recycling strategies. Recent research has shown that there was insufficiently arable land to support small settlements, seriously damaging the countryside and the environment [1]. These phosphate sludges constitute considerable reserves, which are not exploitable by simple washing, because of their low content of P_2O_5 and the abundance of carbonates and silica.

To reduce the quantities of accumulated phosphate sludges (Ps) at ponds and reclaiming the site for other purposes, landfill mining can be considered to be a viable option. Landfill mining is a process by which old solid wastes after excavation and segregation can be considered for further applications. Depending upon the composition, quality of the material, and market demand, many options for reuse are available. Potential reuse of Ps as ceramic products and geopolymer mortar has been widely studied. Phosphorus recovery from phosphate sludge has also met vast attention.

Laboratory studies reported in the literature are limited to the physicochemical characterization of Ps and do not address the effect of long-term storage and their possible contamination potential. Earlier investigations have predominantly highlighted that the accumulation of these sludges which are rich in sediments (carbonates) is not a source of contamination [1]. However, the extent of the acid generation as well as the sources and dynamics of heavy metals (HM) have not been determined so far in phosphate sludges tailings.

The fundamental step to the control and treatment of Ps is to understand their status quo, which normally requires drawing information from environmental monitoring data. The statistical analysis is used as a conventional and prevalent empirical approach to characterize and explore Ps's data. A variety of statistical procedures were used to reveal characteristics and structures within the data, such as principal component analysis (PCA), hierarchical cluster analysis (HCA), and multivariate analysis of variance MANOVA. Also, sequential extraction techniques were carried out to understand the behavior of

heavy metals in Ps as well as static test to evaluate the capacity of acid generation overtime of the mine wastes.

The study deals with Ps of different ages (2018, 2014, and 2009) collected from two ponds. The objective of this work was to determine the main changes over 10 years on the composition of Ps before using them offsite. Multiple characterizations, namely mineralogical, physical and chemical measurements have been made to validate the properties and structural features. Heavy metals concentrations and chemical parameters of the three Ps have been statistically characterized. The study also focuses on the determination of levels of contaminants in Ps in terms of HM mobility and acid generation capacity.

2. MATERIALS AND METHODS

Study areas and sampling. The phosphate sludge storage is located approximately 1.8 km from the washing plant Merah Al Ahrach and 26.8 km southeast of Khouribga, Morocco. The phosphate sludge covers around 40 ha of leasable space. The climate is typically arid and semi-arid over the year. Climatic conditions are generally severe, with the average rainfall of the highest exceeds 187 liters per square meter and the average temperature is around 22 °C. In winter, the mean minimum temperature attains 0 °C and the maximum temperature nearly 40 °C can be reached during the summer.

All samples were collected in February 2018 in the morning from two different ponds. The first pond P1 was built in 2009, the phosphate sludge continued to be accumulated until 2014, and then it was shut down. The second pond P2 was created in 2018 and contains freshly produced sludge. The samples from P1 were collected from the excavated part of the dyke. Two samples were taken from it at the same area and from two depths. The first one was collected at a depth of about 15 m (Ps_{2009}) while the second one was collected at the surface of the dyke (Ps_{2014}). The third sample was taken from the top of P2 (Ps_{2018}). These three samples were yellow and were distinguished by their aspects. The aspect of Ps_{2009} is pasty, Ps_{2014} is fairly brittle and Ps_{2018} is a slurry.

The three Ps samples from each sampling location were collected by chip sampling technique according to the international standard ISO 18400. This procedure involved stratifying every station into regular-sized grid cells and each grid cell was further divided into smaller subcells. Five sampling points in a grid of 5×10 m at each sampling station (4 at the corners and one at the center of the grid) were selected and composite samples consisting of five sub-samples were collected using a plastic spatula. Then the sub-samples are homogenized to obtain a representative sample. On every plot, five soil samples were taken. A total of fifteen samples from the three stations were collected. Samples were taken using a plastic shovel and stored in polyethylene bottles protected from light. All the analyses were conducted following quality assurance and analytical quality control program NM ISO/IEC 17025.

Mineralogical and physical parameters. The samples were examined through X-ray diffraction of Rigaku monochromatized CuK_α radiation (λ = 1.54 Å) using the international standard (EN 13925-2:2003), Fourier transform infrared spectroscopy (FTIR) recorded on KBr pellets Bruker Vertex 70 and their microstructure was performed with a scanning electron microscopy (SEM-SED) EDAX AMETEK (ISO 19702:2016). Density was determined through the pycnometer method (ISO 11272:2017) and the plasticity index using the Atterberg limits methods (ISO 17892-12:2018). The particle size analysis was carried out using a LASER LA-300 HORIBA diffraction granulometry (ISO 13320:2020).

Chemical parameters. Major elements were analyzed by the X-ray fluorescence spectrometry (XRF) technique using a Philips spectrometer (ISO 18227:2014). The differential thermal and thermogravimetric analyses (DTA-TG) were performed under an argon atmosphere with a heating rate of 5 °C/min with instruments SetaramSetsys 24 (ISO 11358-1:2014). The organic matter (*OM*) content of sludge was determined from a 3 g sample, by combustion at 375 °C for 16 h using the international standard (ISO/CD 23265). pH was measured at room temperature (Instruments Hanna HI 2211) (ISO 10390:2005). Electrical conductivity *EC* was determined with HANNA HI 8773 meters (ISO 11265:1994). The cation exchange capacity (*CEC*) was determined by the sodium acetate method [2]. The measured values of *OM*, pH, *EC*, and *CEC* were used in the statistical analysis. Total concentrations of heavy metals in the sludges were determined using a PerkinElmer Optima 3100 RL ICP-AES (ICP) system after the complete digestion of $HNO_3/Br_2/HF/HCl$ (ISO 22036:2009) and are used in the statistical analysis.

Statistical analysis. Descriptive statistics, hierarchical cluster analysis (HCA), principal component analysis (PCA), and multivariate analysis of variance MANOVA were performed using the commercial statistics software package IBM SPSS version 25.0 for Windows.

Sequential extraction. To determine heavy metals mobility, sequential extraction of the heavy metals in the soil samples has been applied as described by Malinowska et al. [3]. Six fractions were obtained: (I) water-soluble, (II) exchangeable, (III) carbonate bound, (IV) Fe and Mn oxide bound, (V) organically bound, and (VI) residual fractions. A brief description of the sequential extraction procedure is presented in Table 1. The sequential extraction was carried out on the three Ps samples. All residues (with exception of fraction VI) were washed with 8 cm^3 of distilled water before proceeding to the next extraction step. The washing water was collected and analyzed together with supernatant from the previous fraction. The supernatant was separated by centrifugation for 30 min at 10 000*g* and removed from the solid residue using a pipette, subsequently filtered again and stocked at 4 °C preceding the analyses. The concentration of heavy metals in each

extract was determined by atomic absorption spectrometry (Perkin Elmer Spectra AA 220 FS) using the international standard (ISO/TS 17073:2013). Each sample was duplicated then analyzed for good repeatability and reproducibility of the measurements.

Table 1

Sequential extraction procedure used in the experiment [3]

Fraction		Procedure
F I	water-soluble	distilled water, r.t.
F II	exchangeable	$MgCl_2$ 1 mol/dm^3, pH 7, NaOH 0.001 mol/dm^3, 1 h, r.t.
F III	carbonate bound	sodium acetate 1 mol/dm^3, pH 5, acetic acid, 1 h, r.t.
F IV	Fe, Mn oxide bound	NH_2OH–HCl 0.004 mol/dm^3 in acetic acid 25 vol. %, r.t.
F V	organically bound	HNO_3 0.02 mol/dm^3, H_2O_2 30 wt. %, pH 2, ammonium acetate 3.2 mol/dm^3 in HNO_3 20 vol. %, r.t.
F VI	residual	digestion in HCl–HNO_3 + HF 150 °C, 2 h

r.t. – room temperature.

Net acid generation pH. Not all sulfides are necessarily available or reactive, and acidity generated by sulfides may be immediately neutralized by carbonate minerals present in the sample, or limited if encapsulated in siliceous hosts, e.g., quartz, plagioclase, etc. Therefore, the static test NAG pH was conducted to determine Ps acid generating potential. The net acid generation (NAG) test directly evaluates the generation of sulfuric acid by the accelerated oxidation of sulfides present in the samples. If the resulting NAG pH was higher than or equal to 4.5 the sample was classified as non-acid-generating. While a sample with a NAG pH lower than 4.5 confirms that sulfide oxidation generates an excess of acidity and classifies the material as higher risk [4].

To perform the NAG pH test, 250 cm^3 of 15% H_2O_2 was added to ca. 2.5 g of the pulverized sample; the suspension was placed inside a fume hood for 24 h and then boiled for 1 h. After cooling to room temperature, the final pH (NAG pH) was recorded.

3. RESULTS AND DISCUSSION

3.1. MINERALOGICAL AND PHYSICAL PARAMETERS

Figure 1 shows the X-ray diffraction patterns and mineral quantification of Ps_{2009}, Ps_{2014}, and Ps_{2018} phosphate sludge samples. The results achieved show the dominance of quartz, calcite, and dolomite. Fluorapatite phases are also present in phosphate sludge. The mineralogical quantification shows that the Ps_{2014} sample has a higher amount of carbonate and silicate than other sludges. Fluorapatite is widespread for all samples.

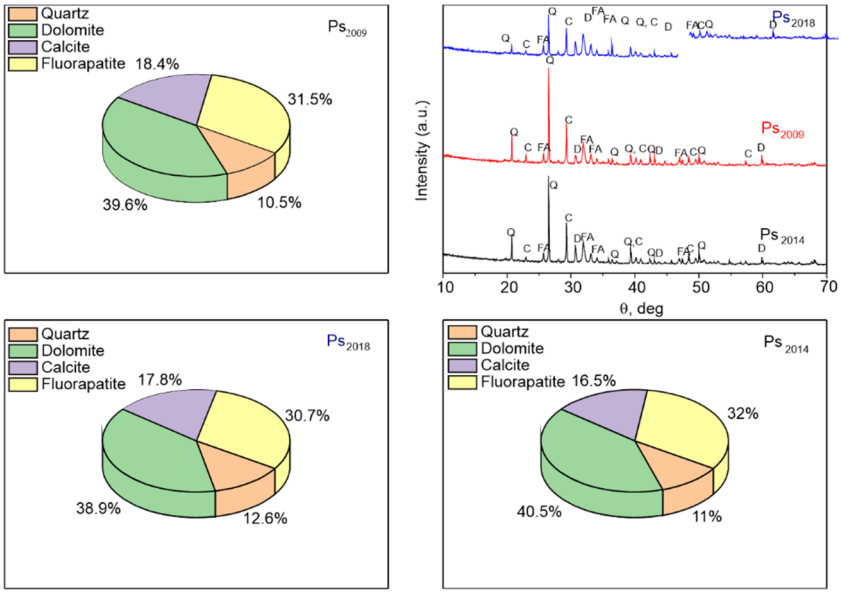

Fig. 1. X-ray diffraction patterns of samples and mineral quantification of Ps_{2014}, Ps_{2009}, and Ps_{2018}

Figure 2 shows the FTIR spectra of the phosphate sludge samples. All spectra are similar and confirm the results of X-ray analysis. The samples contain absorbed H_2O (3400 cm^{-1}) and a principal absorption band at 1430 cm^{-1} corresponding to the dolomite and calcite groups [5]. The bands at 1042.4 cm^{-1} and 473 cm^{-1} are characteristic of fluorapatite and quartz, respectively [6].

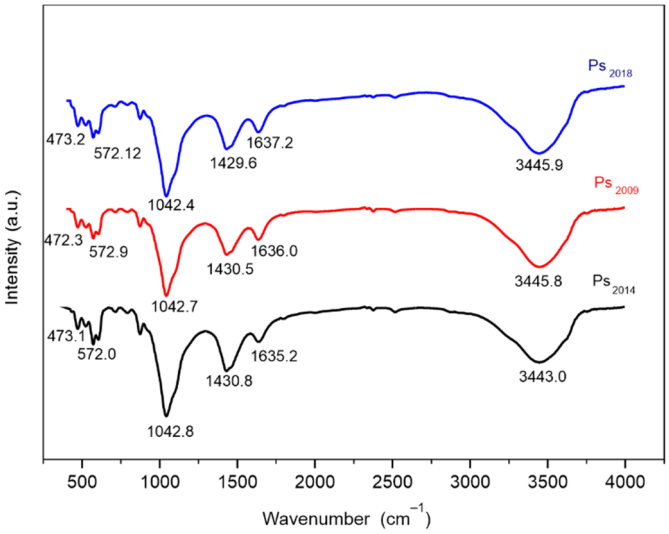

Fig. 2. FTIR Spectra of Ps_{2009}, Ps_{2014}, and Ps_{2018} phosphate sludge samples

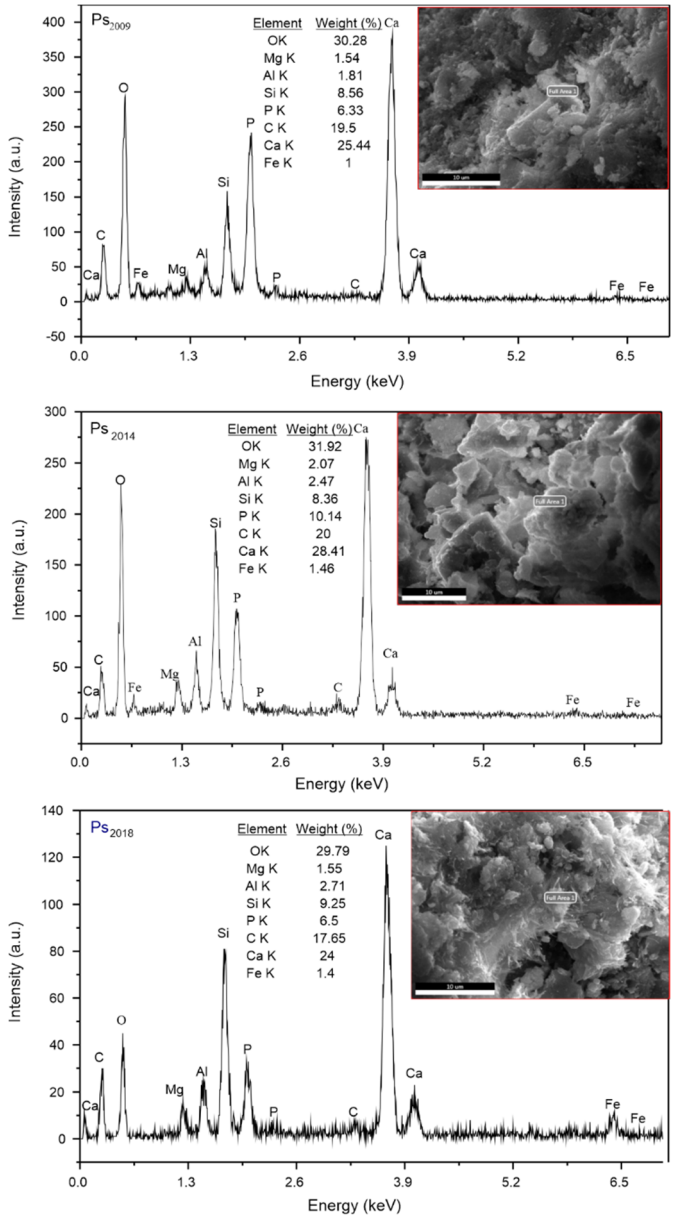

Fig. 3. SEM-EDS analysis of Ps_{2009}, Ps_{2014}, and Ps_{2018} phosphate sludge samples

Scanning electron microscopy (SEM) coupled with elemental analysis (EDAX) was used to determine the structure of the sludge samples (Fig. 3). SEM images show a heterogeneous structure indicating a matrix with not identifiable crystal shapes without bringing a significant change of microstructure arisen from the weather. The EDS shows that Ps_{2014}

is a little richer in C, Ca, Si, and P than Ps_{2009} and Ps_{2018} due to the accumulation of the components of the sludge at the top of tailing ponds. SEM and EDS analysis show a general view of the three samples indicating a matrix, with not identifiable crystal shapes

The measured density varies slightly from 2.81 g/cm^3 to 2.77 g/cm^3 and 2.76 g/cm^3 for Ps_{2014}, Ps_{2009}, and Ps_{2018}, respectively. Accumulation of carbonates in the sludge can give such a value of density. On the other hand, the plasticity index is found to be 9.08, 7.57, and 7.34 for Ps_{2018}, Ps_{2009}, and Ps_{2014}, respectively. The phosphate sludge Ps_{2018} gets more and more saturated with water than other ones, however, under solar drying during several years, it may lose water, which partly explains the lower value of plasticity index for Ps_{2014}.

Table 2

Particle size distribution of phosphate sludge samples [wt. %]

Constituent	Sample		
	Ps_{2014}	Ps_{2009}	Ps_{2018}
Clay (<2 μm)	33.2	34.6	30.5
Fine silt (2–20 μm)	25.29	21.8	24.2
Coarse silt (20–50 μm)	34.59	32.5	33.89
Fine sand (50–200 μm)	6.9	9.98	11.26

Table 2 illustrates the particle size distribution of the samples. The texture is classified in clay, fine and coarse silt, and fine and coarse sand. The texture of the samples is fine, which can be explained by the mining of phosphate rock and processing. Thus, after the extraction technique, the phosphate raw material is sorted according to size and quality. Whilst larger particles over 2 mm get trapped and stored in heaps and the finest particles with a size below 70 μm represent the phosphate washing sludge. The particle size distribution of the three sludges does not show a large variation over time except for the sandy texture. It can be noted that the percentage of fine sand for the Ps_{2018} sample is higher than other ones; meanwhile, the percentage of Ps_{2014} is the lowest. These results do not reflect any changes in the mineralogical and physical composition of Ps over time.

3.2. CHEMICAL PARAMETERS

Different metals present in the phosphate sludge samples were investigated by XRF (Table 3). Sludges predominantly contain carbonates, the Ps_{2014} sample is found to be a little more carbonated than other sludges. The SiO_2 concentrations also show high quartz content. The flotation process contributes to increasing the amount of carbonate and quartz in sludge [7]. The amount of P_2O_5 also depends on the efficiency of the flotation process. Analysis by XRF shows also the presence of low concentrated elements such as Al_2O_3, MgO (<4 wt.%), SO_3 (<2 wt.%), and Fe_2O_3 (<1 wt.%).

Table 3

Mean concentrations of major elements of the phosphate sludge samples [wt. %]

Sample	CaO	SiO_2	P_2O_5	Al_2O_3	MgO	Fe_2O_3	SO_3
Ps_{2014}	35.2	12.7	15.01	3.3	3.0	0.4	1.38
Ps_{2009}	33.5	12.1	14.2	2.54	3.57	0.43	1.35
Ps_{2018}	31.6	15.84	13.5	4.1	3.89	0.99	1.17

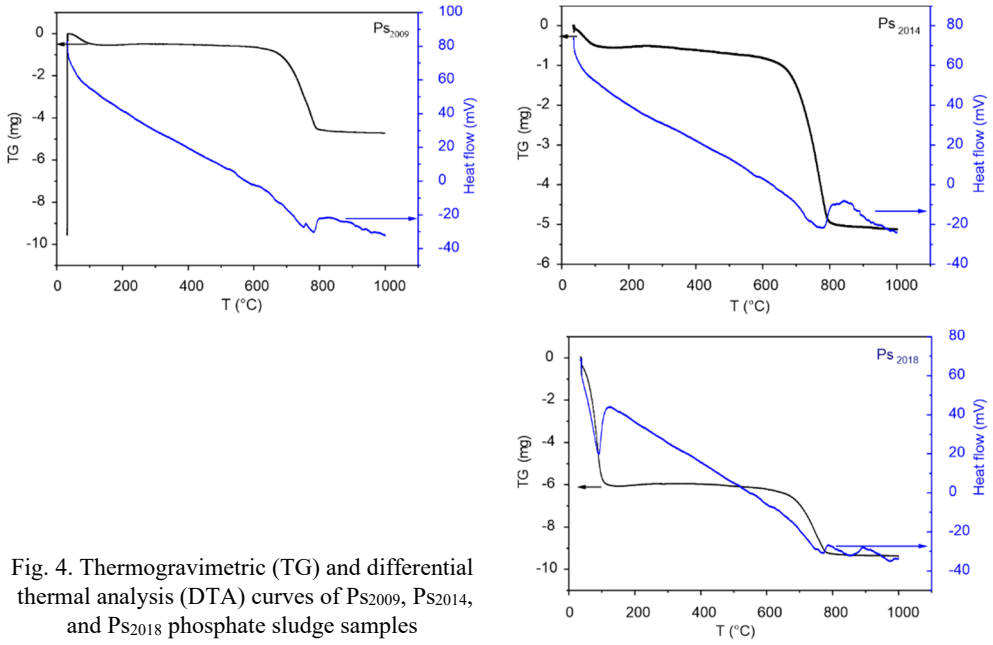

Fig. 4. Thermogravimetric (TG) and differential thermal analysis (DTA) curves of Ps_{2009}, Ps_{2014}, and Ps_{2018} phosphate sludge samples

Thermogravimetric (TG) and differential thermal analysis (DTA) curves of the examined phosphate sludge samples are shown in Fig. 4. The first major weight loss for Ps_{2018}, Ps_{2009}, and Ps_{2014} is located between 100 °C and 200 °C coupled with an endothermic peak at the ATD curve and corresponding to the removal of water absorbed by sludge. We can notice a big difference in this first loss due to the texture of samples: liquid for Ps_{2018}, pasty for Ps_{2009}, and dry for Ps_{2014}. The second weight loss occurs at around 750 °C and 800 °C. This loss corresponds to the decarbonization of carbonates, calcite, and dolomite with the release of CO_2 [8]. Sludge properties analysis shows that solar drying contributes considerably to eliminate the water from the sludge as well as improved via TG/DTA.

3.3. STATISTICAL ANALYSES

To identify the effects of long-term storage on heavy metals concentrations and Ps chemical parameters and determine the most important variables that separate the three

Ps, descriptive statistics, hierarchical cluster analysis (HCA), principal component analysis (PCA), and multivariate analysis of variance MANOVA was performed.

The statistical description of heavy-metal concentrations and chemical parameters in Ps of three different ages are summarized in Tables 4 and 5. The differences between means were determined at the 95% confidence level. Table 4 clearly shows that Zn > Cr > Ni > Pb exhibited high concentrations compared to those of Cd (cf. [9]). Regarding these results, it is obvious that the concentrations of trace metals in the Ps are high. However, chemical parameters vary randomly between samples (Table 5).

Table 4

Statistical description of heavy-metal concentrations [mg/kg]

Ps	Cr			Ni			Pb			Zn			Cd		
	LCB	UCB	Mean	LCB	UCB	Mean	LCB	UCB	Mean	LCB	UCB	Mean	LCB	UCB	Mean
Ps_{2009}	297.84	346.16	322	133.71	158.29	146	38.89	61.11	50	441.74	578.26	510	0.69	1.80	1.25
Ps_{2014}	385.81	432.99	409	154.62	201.38	178	41.24	52.76	47	555.14	683.66	619	0.99	2.08	1.5
Ps_{2018}	483.68	554.72	519	197.34	249.06	223	37.71	52.29	45	722.34	812.06	767	1.03	2.18	1.6

LCB – lower confidence bound, UCB – upper confidence bound.

Table 5

The statistical description of chemical parameters in Ps

Ps	pH			*EC* [µS/cm]			*OM* [mg/g]			*CEC* [cmol·kg^{-1}]		
	LCB	UCB	Mean	LCB	UCB	Mean	LCB	UCB	Mean	LCB	UCB	Mean
Ps_{2009}	7.84	8.55	8.19	238.73	245.93	242.33	2.90	3.78	3.34	4.28	5.14	4.71
Ps_{2014}	7.61	7.96	7.79	253.77	427.47	340.62	5.70	8.19	6.94	4.39	6.42	5.40
Ps_{2018}	7.88	8.35	8.12	284.59	396.60	340.6	2.83	5.25	4.04	3.40	5.77	4.59

EC – electrical conductivity, LCB – lower confidence bound, UCB – upper confidence bound.

Figure 5 displays a boxplot of HM concentrations using statistical description values. The mean values of Cd, Cr, Ni, and Zn in Ps_{2018} are higher than in the other sludges. However heavy metal concentrations in Ps_{2014} are higher than those in Ps_{2009}. This increase resulted from the surface enrichment due to HM accumulations in superficial sludges. The Pb content has a distinctive temporal behavior and it increases over years. However, the high amount of HM in Ps_{2018} and the variation of Pb are highly dependent on the type of the maternal rock, which is their source [9].

Figure 6 displays a boxplot of the variation of pH, *EC*, *CEC*, and *OM* in Ps using statistical description values. The phosphate washing sludge has an alkaline nature (pH ca. 8). This is due to the abundance of minerals such as carbonates in these types of sludge. Also, pH increases over years from 7.79 for Ps_{2014} to 8.2 for Ps_{2009}. The supply and decomposition of organic matter indeed increase the number of negative charges in organic-poor soils. The latter adsorb soil protons and cause an increase in pH [10].

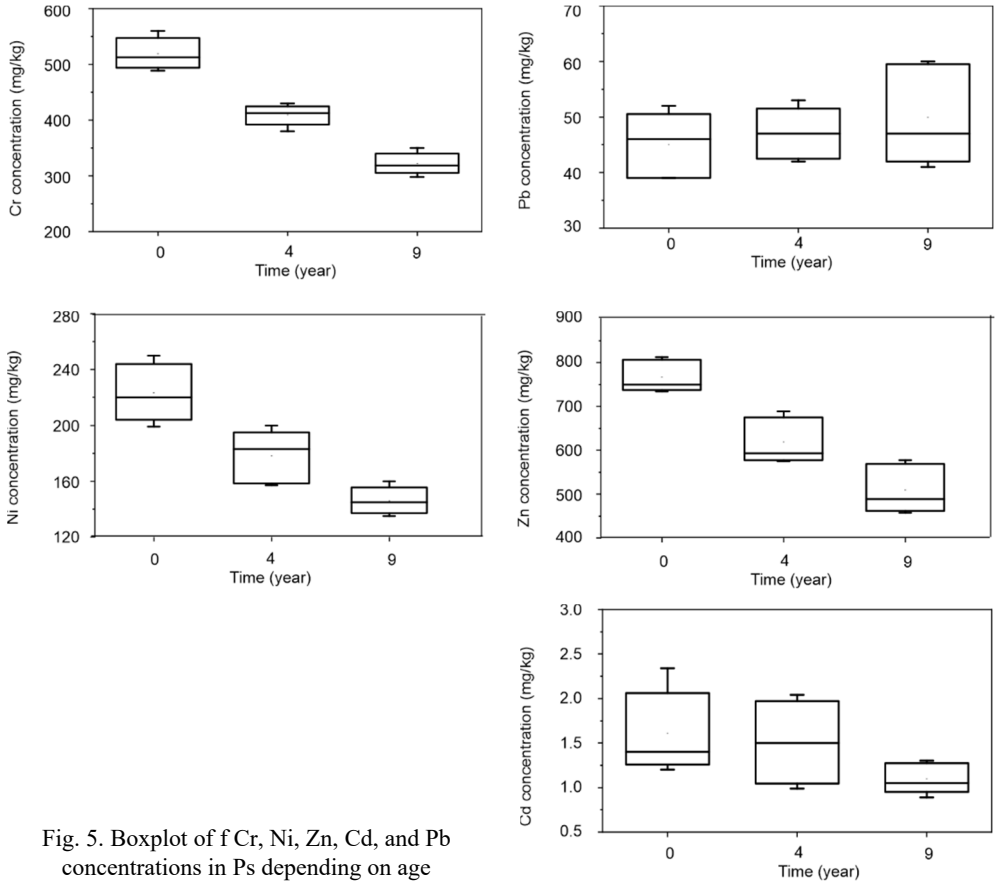

Fig. 5. Boxplot of f Cr, Ni, Zn, Cd, and Pb concentrations in Ps depending on age

Figure 6 displays an increase in the electrical conductivity *EC* over years. The most important increase is observed in the superficial soil layer. Indeed, *EC* of Ps_{2018} (284 µS/cm) as it comes out of the board machine is lower than the conductivity of Ps_{2014} (340.6 µS /cm) and almost equal to Ps_{2009}'s conductivity (242.33 µS /cm). Thus, Ps_{2014} sludge remains under solar radiation exposure, which increases salinity [11].

The organic matter *OM* increased from 4.04 mg/g for Ps_{2018} to 6.9 mg/g for Ps_{2014} and decreased to 3.34 mg/g for Ps_{2009}. The highest values were recorded for the sludge Ps_{2014} in contact with Sun's rays. The microbial activity increases on the surface of ponds due to the release of CO_2 and the consumption of protons, which leads to the biodegradation of organic matter [7].

The sum of hydrolytic acidities and exchangeable bases *CEC* increased from 4.59 to 4.71 and 5.4 $cmol \cdot kg^{-1}$ for Ps_{2018}, Ps_{2009}, and Ps_{2014}, respectively, which is low with a mean value of 4.9 $cmol \cdot kg^{-1}$. This increase could be attributed to the accumulation of materials bearing a negative charge, and the variation of organic matter contents [12, 13].

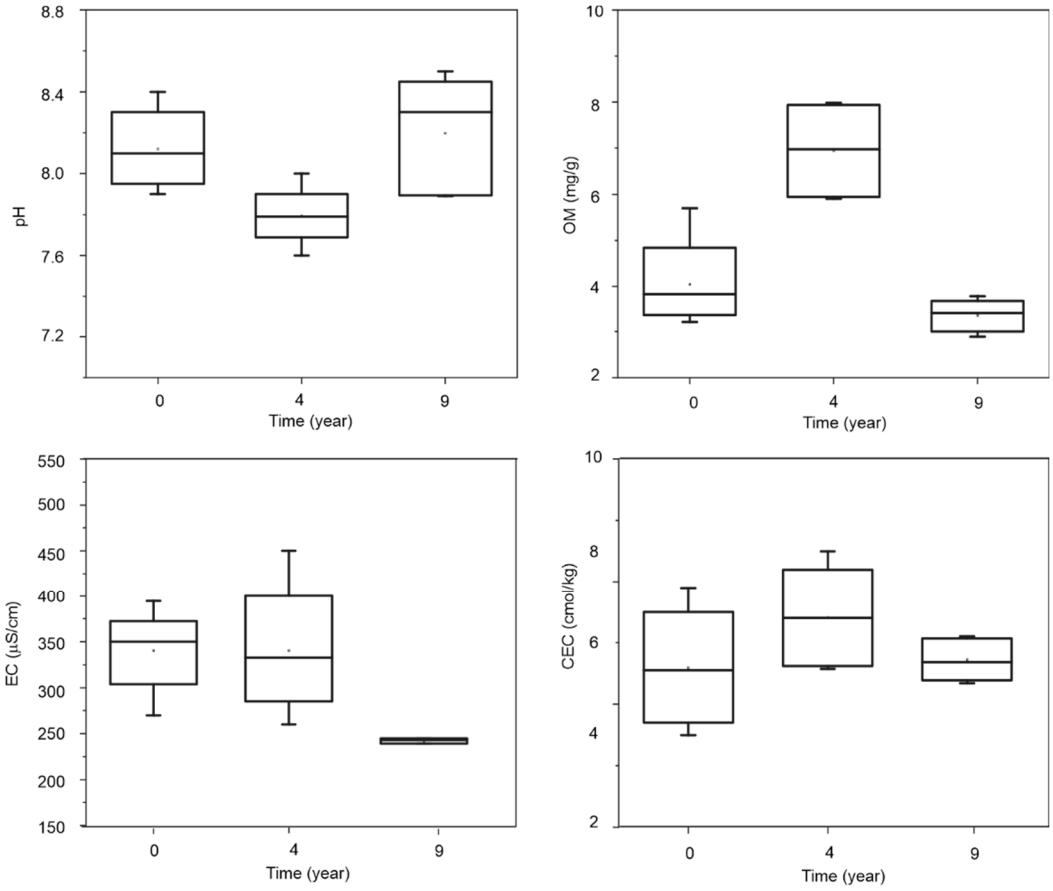

Fig. 6. Boxplot of pH, *EC*, *CEC*, and *OM* in Ps depending on age

To evaluate the similarities and differences of the three Ps samples, hierarchical cluster analysis (HCA) was applied. HCA for the identification of homogeneous subgroups of phosphate sludges was developed according to Ward's method [14].

In the current study, HCA was performed among fifteen Ps samples (1–15) without taking into account variable age. Results are shown in a dendrogram (Fig. 7) where steps in the hierarchical clustering solution and values of the distances between clusters are represented.

The three obtained clusters correspond perfectly to Ps_{2009}, Ps_{2014}, and Ps_{2018}. This result shows that there is a significant difference between the three populations of samples. This means that samples from every cluster have the same origins. The three clusters C1, C2, and C3 correspond respectively to Ps_{2009}, Ps_{2014}, and Ps_{2018}.

The total number of variables characterizing our samples is nine and they can be divided into two categories: HM concentrations and chemical parameters. To assess the differences

between our fifteen samples and also to detect the structure in the relationships of the nine variables, we opted for a factorial method of reducing dimension: the PCA analysis.

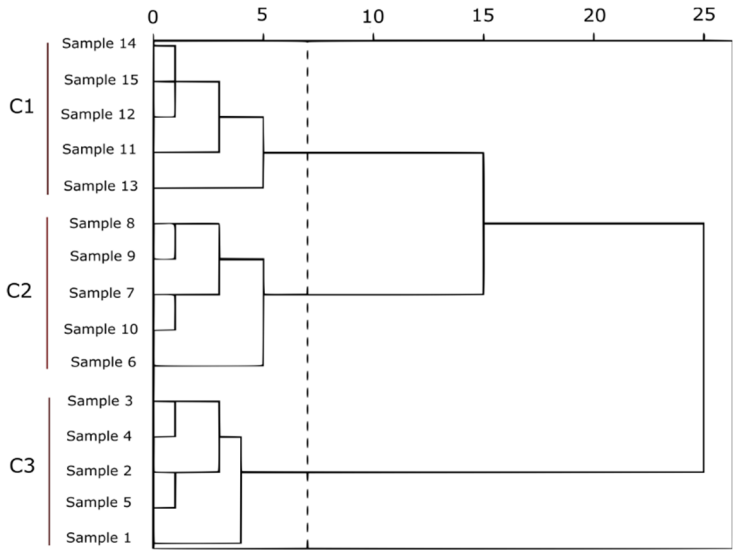

Fig. 7. Dendrogram obtained by hierarchical clustering analysis of Ps data

The PCA is widely used to reduce data and to extract a smaller number of independent factors (principal components) for analyzing relationships among observed variables. This analysis involves a mathematical procedure to transform the original set of correlated variables with high dimensionality into a much smaller subset of uncorrelated variables called principal components (PCs). The original variables were transformed to PCs using eigenanalysis, and the eigenvalues show the variance of each component. Principal components are those whose eigenvalues exceed 1 [15]. Varimax with Kaiser normalization was used as the rotation method. The PCs were extracted based on eigenvalues (eigenvalues >10% and total PCs >70%) [16].

In this study, PCA is used two times: to evaluate the behavior of HM concentrations and a second time to assess the changes in chemical parameters over time.

Table 6

The results of the principal component analysis of HM in phosphate sludges

Component	Eigenvalue	% variance	The sum of squared loadings		
1	2.914	58.287	2.914	58.287	58.287
2	0.956	77.405	0.956	19.118	77.405
3	0.897	95.354	–	–	–
4	0.143	98.207	–	–	–
5	0.090	100.000	–	–	–

The PCA of HM concentrations leads to a reduction of the initial dimension of the data set from five to two components which explain 77.4% of the data variation as shown in Table 6. The relations among the heavy metals based on the first two principal components are illustrated in Fig. 8 in two-dimensional space.

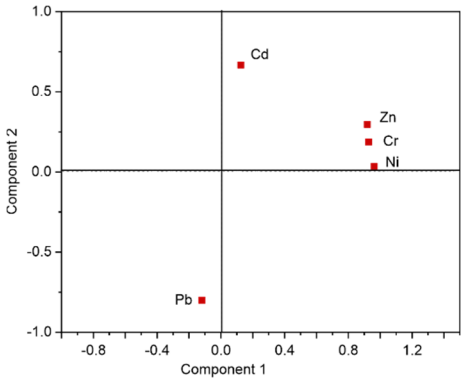

Fig. 8. Two-dimensional principal component loading plot of HM concentration

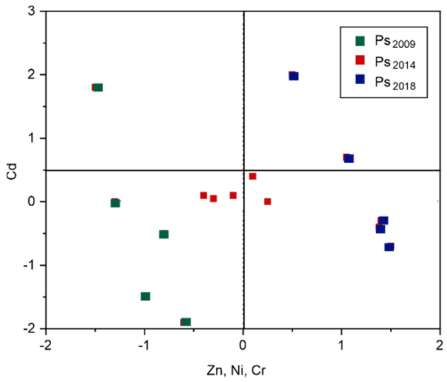

Fig. 9. Two-dimensional principal component loading plot of Ps_{2018}, Ps_{2014}, and Ps_{2009} using PCA results of HM concentrations

The first PC, which was called PC1, accounted for 58.28% of the total variance and was positively and strongly related to Zn, Ni, and Cr whose coefficients were 0.919, 0.962, and 0.928, respectively (Table 7). The significant correlation among Zn, Ni, and Cr indicated that these three HM have a common anthropogenic source and have similar properties, which explains their similar behavior over time. The PC2, which accounted for 77.405% of the total variance, was positively related to Cd and negatively related to Pb (the PC2 coefficients of which were 0.667 and –0.801, respectively). Pb shows negative correlations with Cd, implying that they have an opposite behavior due to accumulation in a relatively long-term period [9, 17].

Table 7

PCA loadings of heavy metals
on significant Varimax rotated principal components

Elements	PC1	PC2
Cr	0.928	0.187
Ni	0.962	0.034
Pb	–0.119	–0.801
Zn	0.919	0.296
Cd	0.125	0.667

The two principal components PC1 and PC2 can separate well the three sludges one from each other as shown in Fig. 9. Ps_{2018} is richer in Cd, Cr, Ni, and Zn than the other

sludges due to the origin of the mother material. However, Ps_{2014} is richer than Ps_{2009} in heavy metals due to superficial accumulation.

Table 8

The results of the principal component analysis of Ps samples

Component	Eigenvalue	% variance	Sum of squared loadings		
1	1.954	48.857	1.954	48.857	48.857
2	1.017	74.273	1.017	25.417	74.273
3	0.726	92.433	–	–	–
4	0.303	100.000	–	–	–

The PCA of Ps chemical parameters leads to a reduction of the initial dimension of the data set from four to two components which explain 74.27% of the data variation as shown in Table 8. The relations among pH, *EC*, *CEC*, and *OM* based on the first two principal components are illustrated in Fig. 10 in two-dimensional space.

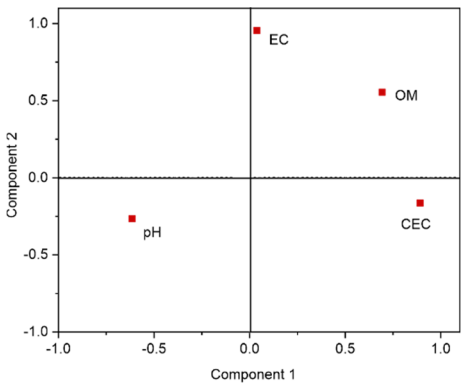

Fig. 10. Two-dimensional principal component loading plot of Ps chemical parameters

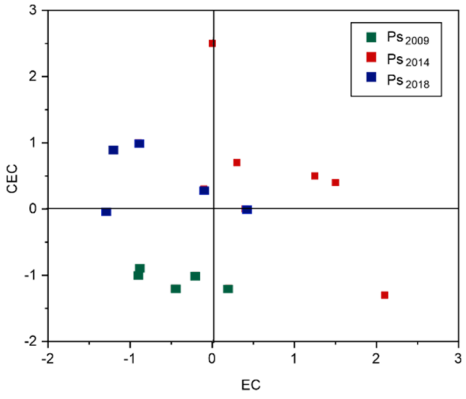

Fig. 11. Two-dimensional principal component loading plot of Ps_{2018}, Ps_{2014}, and Ps_{2009} using PCA results of Ps chemical parameters

The PC1 accounted for 48.857% of the total variance and was positively related to *OM* and *CEC* whose coefficients were 0.693 and 0.891, respectively (Table 9). The PC1 shows also a strong negative correlation with pH whose coefficient was –6.14. These results indicate that *OM* and *CEC* have the same behavior over years and an opposite behavior with pH due to biodegradation of organic matter. The PC2 accounted for 74.273% of the total variance and was strongly related to *EC* and moderately related to *OM* whose coefficients were 0.955 and 0.555, respectively. Solar radiation exposure explains their similar behavior over years. The plot of the parameters of Ps according to PC1 and PC2 shows a separation of the three sludges as shown in Fig. 11. The Ps_{2018} has high values of *OM*, *EC*, and *CEC* higher than Ps_{2018} and Ps_{2009}. However, we can see

that Ps_{2018} has the highest value of pH. These results confirm PCA of Ps chemical parameters and indicate that these sludges change over time due to their exposition to Sun's radiation.

Table 9

PCA loadings of chemical parameters
on significant varimax rotated principal components

Parameter	PC1	PC2
pH	–0.614	–0.266
EC	0.038	0.955
OM	0.693	0.555
CEC	0.891	–0.164

Statistical analysis PCA and HCA indicate that there are three sources responsible for the behavior of Ps over years: common origin and accumulation of HM and solar radiation exposure. It is important to identify the relative contribution of HM concentrations and chemical parameters for distinguishing the three sludges. To investigate the interelement relationship in Ps over years and to study the significance of the similarities and differences between groups of variables (HM concentrations and chemical parameters). MANOVA method is applied with a multiple comparison test.

Multivariate methods are useful where several dependant variables (p) are measured on each sampling unit instead of one variable. In our study, Ps's data are used for analyzing if long-term storage has a statistically significant effect on HM concentrations and chemical parameters.

Table 10

Inter-element effects for HM concentrations and chemical parameters in Ps

Dependent variable	Degrees of freedom	Mean square	Ratio of residual variance	Significance
Cr	2	48818.867	94.033	0.000
Ni	2	7522.400	25.465	0.000
Pb	2	31.667	0.699	0.516
Zn	2	83304.200	35.674	0.000
Cd	2	0.170	0.809	0.468
pH	2	0.230	4.971	0.027
EC	2	16097.937	6.964	0.010
OM	2	18.267	26.381	0.000
CEC	2	0.968	1.708	0.222

The results of inter-elements effects tests obtained with MANOVA of the phosphate sludges are shown in Table 10. The hypothesis testing in the following analysis is based

on a 0.05 significance level. According to these results, the Cr, Ni, and Zn are significantly influenced by long-term storage ($p < 0.05$). Also, this result indicates that pH, *EC*, and *OM* are significantly influenced by age ($p < 0.05$). Meanwhile, Cd, Pb, and *CEC* did not vary significantly ($p > 0.05$) from one year to another.

Table 11

Test results for HM concentrations in Ps_{2018}, Ps_{2014}, and Ps_{2009}

Sludge		Dependent variables									
		Cr		Ni		Pb		Zn		Cd	
I	*J*	*I-J*	*P*	*I-J*	*P*	*I-J*	*P*	*I-J*	*P*	*I-J*	*P*
Ps_{2009}	Ps_{2014}	–87.40*	0.000	–32.00*	0.012	3.00	0.495	–109.4	0.004	–0.2560	0.395
	Ps_{2018}	–197.20*	0.000	–77.20*	0.000	5.00	0.263	–257.20*	0.000	–0.3580	0.241
Ps_{2014}	Ps_{2009}	87.40*	0.000	32.00*	0.012	–3.00	0.495	109.40*	0.004	0.2560	0.395
	Ps_{2018}	–109.80*	0.000	–45.20*	0.001	2.00	0.647	–147.80*	0.000	–0.1020	0.731
Ps_{2018}	Ps_{2009}	197.20*	0.000	77.20*	0.000	–5.00	0.263	257.20*	0.000	0.3580	0.241
	Ps_{2014}	109.80*	0.000	45.20*	0.001	–2.00	0.647	147.80*	0.000	0.1020	0.731

I-J – mean difference, *P* – significance. * indicates a 0.05 significance level.

Table 12

Test results for chemical parameters in Ps_{2018}, Ps_{2014}, and Ps_{2009}

Sludge		Dependent variables							
		pH		*EC*		*OM*		*CEC*	
I	*J*	*I-J*	*P*	*I-J*	*P*	*I-J*	*P*	*I-J*	*P*
Ps_{2009}	Ps_{2014}	0.4040*	0.012	–98.29*	0.007	–3.6040*	0.000	–0.6900	0.173
	Ps_{2018}	0.0780	0.577	–98.268*	0.007	–0.6980	0.209	0.1280	0.793
Ps_{2014}	Ps_{2009}	–0.4040*	0.012	98.2900*	0.007	3.6040*	0.000	0.6900	0.173
	Ps_{2018}	–0.3260*	0.034	0.0220	0.999	2.9060*	0.000	0.8180	0.111
Ps_{2018}	Ps_{2009}	–0.0780	0.577	98.2680*	0.007	0.6980	0.209	–0.1280	0.793
	Ps_{2014}	0.3260*	0.034	–0.0220	0.999	–2.9060*	0.000	–0.8180	0.111

I-J – mean difference, *P* – significance. * indicates a 0.05 significance level.

Tables 11 and 12 show the multiple comparison test results obtained with MANOVA analysis for HM concentrations and chemical parameters of the three phosphate sludges. It is evident from the results of the test that Pb, Cd, and *CEC* have no significant variation between the three Ps. However, concentrations of Cr, Ni, and Zn exhibit strong and significant differences with age due to the origin of Ps's mother rock. For pH, *OM* and *EC*, no significant variation is observed between Ps_{2018} and Ps_{2009} which suggests that these three parameters might be affected by some other sources.

These results are in agreement with those obtained with PCA and HCA. MANOVA analysis shows that long-term storage has a significant impact on Cr, Ni, and Zn contents. Moreover, this analysis shows a significant variation only in pH, *OM*, and *EC* of sludges exposed to the sun's rays.

It can be concluded that parameters such as Sun's ray exposition, geo-accumulation, and the mother rock origin influence the behavior of Ps over the year. This statistical study could be considered as a contribution to the knowledge and rational management of the Ps ponds.

3.4. SEQUENTIAL EXTRACTIONS

To evaluate the relative distribution of the five HM (Cd, Ni, Zn, Cr, and Pb) in a soluble, exchangeable carbonate bound, reducible (Fe-Mn oxide), organic and sulfide, and residual fractions, a sequential extraction procedure is used. Sequential extraction is more and more commonly used and recommended for testing soils contaminated with heavy metals and for testing waste containing elevated content of these elements [3]. Contrary to the determination of the total heavy metal content in Ps, the sequential extraction procedure provides interesting information on metal mobility.

The three sludges were subjected to extraction by the six-step sequential extraction procedure. The concentration of heavy metals in fractions of Ps_{2009}, Ps_{2014}, and Ps_{2018} is shown in Table 13. For all HM, the sum of six fractions is in good agreement with their total concentration, which confirms the validity and reliability of the obtained results. The number of heavy metals extracted with distilled water was very low and did not exceed 5% of the total content. In all other fractions, the concentration of heavy metals varied between the three different sludges.

In the three samples Ps_{2009}, Ps_{2014} and Ps_{2018}, Cd was mainly present in the residual fraction (>50%) and the fraction bound to Fe and Mn (>25%) oxides. Qiao et al. [18] explained this distribution of Cd by its incorporation in mineral silicate and its inclusion in oxide minerals. The phosphate sludges storage had no significant effects on the distribution of Cd in the different soil fractions, which should be related to the low Cd content of the Ps.

The chemical fractionation indicated that Pb was predominantly present in the residual fraction (>56%) and the fraction bound to Fe and Mn (>20%) oxides in the three samples. The distribution of Pb in the soil fractions is mainly the same in the Ps. The majority of Ni existed in the residual fraction (>80%) for all the samples. These results were confirmed by Dong et al. [19] who generally stated that Ni is mainly in a detrital form in soils and sediment. The storage of phosphate sludges did not have any effect on the distribution of Ni between the different soil fractions.

Cr was found in the residual fraction (>60%) and bound to Fe and Mn oxides (>25%). The storage of phosphate sludges, however, significantly increased the concentration of Cr bound to carbonates and in the residual fraction, which confirms the relatively low availability of Cr [20].

The majority of Zn existed in the residual fraction for all the samples (>88%). The sequential extractions indicated that the phosphate sludges storage increased the relative

amount of Zn bound to Fe and Mn oxides (F IV) and slightly the concentration of Zn bound to the organic matter fraction (F V). However, this storage significantly increased the relative amount of Zn in easily extractable fractions (water-soluble, exchangeable, and bound to carbonates). Indeed, the Zn availability is influenced by the total Zn content, the pH, the organic matter content, the availability of adsorption sites, and the microbial activity in the soil. This increase is mainly due to the effect of pH, which is considered a very important factor for the mobility and the bioavailability of Zn in amended soils. A pH increase results in a decrease of the Zn bioavailability in soils, whereas a decrease of the pH in the soil solution increases the solubility of Zn [3].

Table 13

Heavy metal fractions in Ps_{2009}, Ps_{2014}, and Ps_{2018} samples [mg/kg dry mass]

Bound	Cr	Ni	Pb	Zn	Cd
Ps_{2009}					
Watersoluble F I	196.42	4.38	2.5	10.2	0.0655
Exchangeable F II	14.49	4.205	2.001	7.4	0.039
Carbonate bound F III	9.66	2.5	3.9	5.7	0.07
Fe, Mn oxide bound F IV	6.44	11.684	12.5	50	0.327
Organically bound F V	83.72	4.38	3.5	11.73	0.026
Residual F VI	12.88	116.8	28.5	423.3	0.799
Ps_{2014}					
Watersoluble F I	18.405	5.34	2.31	12.38	0.075
Exchangeable F II	12.27	1.787	1.88	9.285	0.045
Carbonate bound F III	8.18	8.9	3.76	6.19	0.09
Fe, Mn oxide bound F IV	106.34	14.24	11.75	61.9	0.375
Organically bound F V	16.39	5.34	2.82	14.237	0.03
Residual F VI	249.01	142.4	26.79	513.3	0.915
Ps_{2018}					
Watersoluble F I	23.12	6.69	2.25	15.34	0.08
Exchangeable F II	15.511	2.23	1.89	11.5	0.048
Carbonate bound F III	10.38	11.15	3.6	7.61	0.096
Fe, Mn oxide bound F IV	134.95	17.84	11.25	76.71	0.4
Organically bound F V	20.75	6.69	2.7	17.65	0.032
Residual F VI	316.3	178.4	25.4	636.62	0.976

Based on the results obtained in this study, the most relative significance of Cr, Pb, Cd, Ni, and Zn fractions in the three Ps is the residual fraction followed by the fraction bound to Fe and Mn which are the immobile fractions. This demonstrated their stronger stability and lower environmental risk [21].

3.5 HEAVY METALS MOBILITY

Heavy metals in the exchangeable and carbonate-bound fractions are considered easily mobile and thus represent a potential risk for the environment, while the reducible and oxidizable fractions are relatively stable. The residual fraction represents the least-mobile fraction. The mobility of HM is defined by their capacity to pass into soil compartments where they are less energetically retained. It depends on many factors that are related to the nature of the element and the soil properties (e.g., pH, clay content, organic matter rate) [22].

To evaluate HM mobility in soil, researchers have used the relative index, which was calculated as a mobility factor (*MF*) based on heavy metal in the mobile fraction to the sum of all fractions. If *MF* is high, it indicates that the metal is in a state of high mobility, and consequently, its availability to the biological systems will be high [23]. The mobility factor (*MF*) is calculated by the following equation:

$$MF = \frac{\text{F I} + \text{F II} + \text{F III}}{\text{F I} + \text{F II} + \text{F III} + \text{F IV} + \text{F V} + \text{F VI}} \times 100\%$$

where the description of the fractions is given in Table 1 (cf. also Table 13).

The MF of the studied heavy metals show the following trend: Cd > Zn > Ni > Pb > Cr and did not exceed 23% in the three phosphate sludges (Table 14).

Table 14

Mobility factors (*MF*) for heavy metals of Ps_{2009}, Ps_{2014}, and Ps_{2018} samples

Metal	Ps_{2009}	Ps_{2014}	Ps_{2018}
Cr	2.14	1.26	1.29
Ni	7.3	7.02	7.26
Pb	6.38	5.76	5.91
Zn	8.6	11.08	11.98
Cd	20.9	18.3	22.7

The phosphate sludges storage during 10 consecutive years had no important effect on the mobility of heavy metals. This confirmed that Zn, Pb, Ni, and Cr were very stable in the soil surface horizons and that the Ps storage does not cause a huge heavy metal mobilization. Cadmium is found to be the most mobile metal in the soil since it has a mobility factor of 18.3, 20.9, 22.7% for Ps_{2014}, Ps_{2009}, and Ps_{2018}, respectively (Table 14). However, this sludge doesn't represent a risk to the environment. Recent research shows that heavy metal fractions are bound to carbonates, which hampers their immigration to depths of tens of centimeters [12, 13, 24]. Indeed, at elevated pH, the presence of carbonates in the soil leads to an increase in the retention of heavy metals. When the carbonate content and the pH are high, heavy metals are retained in the soil mainly as carbonate salts [25].

pH values obtained at the end of the NAG test (final NAG pH) are 6.94, 7.69, and 7.51 for Ps_{2014}, Ps_{2009}, and Ps_{2018}, respectively. The three values are greater than 4.5 in all samples. According to this, the studied Ps are classified as non-acid-generating, indicating that they are not generating acidic drainage when exposed to atmospheric conditions over years.

4. CONCLUSIONS

In this work, phosphate sludges (Ps) of different ages were studied. After more than 10 years of exposure to surficial conditions, sludge accumulated in tailing dykes in Khouribga's Morocco phosphate mine has been hardly weathered.

The X-ray fluorescence, FTIR, and SEM-EDS analysis show that the sludge is composed especially of carbonate, silicate, and fluorapatite but they did not reveal any changes over time. Texture effects can be achieved by the strong influence of natural drying on the superficial sludges. Thus, the weather, mostly sunny most of the time, reduces their pH value and plasticity index but increases the conductivity and organic matter. However, their *CEC* remains unchanged. XRF shows that Ps are highly carbonated with an average concentration of 13.5 and 14.2 wt. % for SiO_2 and P_2O_5, respectively. The accumulation of sludges throughout the years was found to increase the content of major elements.

Descriptive statistics and HCA study of heavy-metal concentrations and chemical parameters pH, *OM*, *EC*, and *CEC* indicate that the three Ps are different. PCA and MANOVA show that there are three sources responsible for the behavior of Ps over years which are mother rock origin and accumulation of HM and solar radiation exposure.

The sequential extraction procedure is used to evaluate the relative distribution of the five HM (Cd, Ni, Zn, Cr, and Pb) in a soluble, exchangeable, carbonate bound, reducible (Fe-Mn oxide), organic and sulfide, and residual fractions. The distribution of heavy metals between the different fractions in Ps showed the residual fraction to be dominant, followed by the fractions bound to Fe and Mn oxides, which represent the least-mobile fractions. The mobility factor (*MF*) was quite low and did not change after 10 years of storage. Also, the net acid generation pH for the three samples was greater than 4.5 classifying the Ps as non-acid-generating over time.

Overall, it can be concluded that Ps offer significant potential for reuse because of their availability in large quantities in ponds. This variation in parameters may have an impact on the decision and the choice of methods for the final application of the phosphate sludge. The results of this study could serve as a reference database to assess the future behavior of Ps for reuse. Furthermore, this work could be used to verify the possible impact that a Ps might have in the future.

ACKNOWLEDGEMENTS

The authors thank the anonymous reviewer for his/her valuable comments.

REFERENCES

[1] HASAN S.N.M.S., KUSIN F.M., JUSOP S., YUSUFF F.M., *Potential of soil, sludge and sediment for mineral carbonation process in Selinsing Gold Mine, Malaysia*, Miner., 2018, 8 (6), 257. DOI: 10.3390/min 8060257.

[2] JAREMKO D., KALEMBASA D., A *Comparison of methods for the determination of cation exchange capacity of soils*, Ecol. Chem. Eng. S, 2014, 21 (3), 487–498. DOI: 10.2478/eces-2014-0036 (in Polish).

[3] MALINOWSKA E., *Zinc speciation in soil under various rates of sewage sludge and liming*, Environ. Prot. Eng., 2016, 42 (4), 5–15. DOI: 10.5277/epe160401.

[4] OH C., JI S., YIM G., *Evaluation of net acid generation pH as a single indicator for acid forming potential of rocks using geochemical properties*, Environ. Monit. Assess., 2017, 189 (4), 165. DOI: https: //doi.org/10. 1007/s10661-017-5869-7.

[5] SOLOTCHINA E.P., SOLOTCHIN P.A., *Composition and structure of low-temperature natural carbonates of the calcite-dolomite series*, J. Struc. Chem., 2014, 55 (4), 779–785. DOI: 10.1134 /s00224766 14040295.

[6] ZHAI S., SHIEH S.R., XUE W., XIE T., *Raman spectra of stronadelphite $Sr_5(PO_4)_3F$ at high pressures*, Phys. Chem. Miner., 2015, 42 (7), 579–585. DOI: 10.1007/s00269-015-0745-x.

[7] COLLARD M., TEYCHENÉ B., LEMÉE L., *Comparison of three different wastewater sludge and their respective drying processes: Solar, thermal and reed beds. Impact on organic matter characteristics*, J. Environ. Manage., 2017, 203 (2), 760–767. DOI: 10.1016/j.jenvman.2016.05.070.

[8] ARGANE R., BENZAAZOUA M., BOUAMRANE A., HAKKOU R., *Cement hydration and durability of low sulfide tailings-based renders. A case study in Moroccan constructions*, Miner. Eng., 2015, 76 (1), 97–108. DOI: 10.1016/j.mineng.2014.10.022.

[9] WOŁEJKO E., WYDRO W., BUTAREWICZ A., LOBODA T., *Effects of sewage sludge on the accumulation of heavy metals in soil and in mixtures of lawn grasses*, Ecol. Chem. Eng. A., 2013, 19 (10), 1199–1210. DOI: 10.2428/ecea.2012.19 (10)114.

[10] DALDOUL G., SOUISSI R., SOUISSI F., JEMMALI N., CHAKROUN H.K., *Assessment and mobility of heavy metals in carbonated soils contaminated by old mine tailings in North Tunisia*, J. Afr. Earth. Sci., 2015, 110, 150–159. DOI: 10.1016/j.jafrearsci.2015.06.004.

[11] GENG Y., KHODADADI H., KARIMIPOUR A., REZA S.M., NGUYEN T.K., *A comprehensive presentation on nanoparticles electrical conductivity of nanofluids. Statistical study concerned effects of temperature, nanoparticles type and solid volume concentration*, J. Phys. A, 2019, 542, 1–24. DOI: 10.1016/j.physa. 2019.123432.

[12] GUSIATIN Z.M., KULIKOWSKA D., *Behaviors of heavy metals (Cd, Cu, Ni, Pb and Zn) in soil amended with composts*, Environ. Techn., 2016, 37 (18), 2337–2347. DOI: 10.1080/09593330. 2016.1150348.

[13] AFSANEH M., NABIOLLAH M., FARAMARZ M., ALI R.V., *Distribution and ecological risk assessment of heavy metals in roadside soil along the hemmat highway of Tehran, Iran*, Environ. Prot. Eng., 2018, 44 (3), 5–17. DOI: 10.37190/epe180301.

[14] ZUMLOT T., BATAYNEH A., NAZAL Y., GHREFAT H., MOGREN S., ZAMAN H., ELAWADI E., LABOUN A., QAISY S., *Using multivariate statistical analyses to evaluate groundwater contamination in the northwestern part of Saudi Arabia*, Environ. Earth. Sci., 2013, 70 (7), 3277–3287. DOI: 10.1007 /s12665 -013-2392-1.

[15] MA L., SUN J., YANG Z., WANG L., *Heavy metal contamination of agricultural soils affected by mining activities around the Ganxi River in Chenzhou, Southern China*, Environ. Monit. Assess., 2015, 187 (12), 731–740. DOI: 10.1007/s10661-015-4966-8.

[16] LI J., PU L., LIAO Q., ZHU M., DAI X., XU Y., JIN Y., *How anthropogenic activities affect soil heavy metal concentration on a broad scale: a geochemistry survey in Yangtze River Delta, Eastern China*, Environ. Earth. Sci., 2014, 73 (4), 1823–1835. DOI: 10.1007/s12665-014-3536-7.

[17] KOUIDRI M., DALI Y.N., BENABDELLAH I., GHOUBALI R., BERNOUSSI A., LAGHA A., *Enrichment and geoaccumulation of heavy metals and risk assessment of sediments from coast of Ain Temouchent (Algeria)*, Arab. J. Geosci., 2016, 9 (5), 354–363. DOI: 10.1007/s12517-016-2377-y.

[18] QIAO Y.M., YANG Y., GU J.G., ZHAO J.G., *Distribution and geochemical speciation of heavy metals in sediments from coastal area suffered rapid urbanization, a case study of Shantou Bay, China*, Mar. Pollut. Bull., 2013, 68 (1–2), 140–146. DOI: 10.1016/j.marpolbul.2012.12.003.

[19] DONG B., LIU X.G., DAI L.L., DAI X.H., *Changes of heavy metal speciation during high-solid anaerobic digestion of sewage sludge*, Bioresour. Technol., 2013, 131 (2013), 152–158. DOI: 10.1016 /j.biortech.2012.12.112.

[20] ANJU M., BANERJEE D.K., *Comparison of two sequential extraction procedures for heavy metal partitioning in mine tailings*, J. Chemosphere, 2010, 78 (2010), 1393–1402. DOI: 10.1016 /j.chemo sphere. 2009.12.064.

[21] JUN R., ZHEN S., LING T., JIANXIU H., *Speciation and contamination assessment of metals in the sediments from the lanzhou section of the Yellow River*, China, Environ. Prot. Eng., 2017, 43 (3), 113–124. DOI: 10.5277/epe170307.

[22] SHIM J., SHEA P.J., OH B.T., *Stabilization of heavy metals in mining site soil with silica extracted from Corn Cob*, Water. Air. Soil. Pollut., 2014, 225 (10), 2152–2164. DOI: 10.1007/s 11270-014-2152-1.

[23] ZHENG S., ZHANG M., *Effect of moisture regime on the redistribution of heavy metals in paddy soil*, J. Environ. Sci., 2011, 23 (3), 434–443. DOI: 10.1016/s1001-0742 (10)60428-7.

[24] KATOH M., WANG Y., KITAHARA W., SATO T., *Impact of phosphorus and water-soluble organic carbon in cattle and swine manure composts on lead immobilization in soil*, Environ. Techn., 2015, 36 (15), 1943–1953. DOI: 10.1080/09593330.2015.1016461.

[25] MALLAMPATI S.R., MITOMA Y., OKUDA T., SAKITA S., KAKEDA M., *Enhanced heavy metal immobilization in soil by grinding with addition of nanometallic Ca/CaO dispersion mixture*, J. Chemosphere, 2012, 89 (6), 717–723. DOI: 10.1016/j.chemosphere.2012.06.030.